



METIS

Seismic Risk Assessment
for Nuclear Safety

Research & Innovation Action

NFRP-2019-2020

Summary of WP4 activities and insights

Deliverable D4.7

Version N°1.0

Authors:

Marco Pagani, Anna Rood, Marco Pilz, Graeme Weatherill, Luis Guillermo Alvarez Sanchez, Saran Srikanth Bodda & METIS WP4 participants



This project has received funding from the Horizon 2020 programme under grant agreement n°945121. The content of this presentation reflects only the author's view. The European Commission is not responsible for any use that may be made of the information it contains.



Disclaimer

The content of this deliverable reflects only the author's view. The European Commission is not responsible for any use that may be made of the information it contains.



Document Information

Grant agreement	945121
Project title	Methods And Tools Innovations For Seismic Risk Assessment
Project acronym	METIS
Project coordinator	Dr. Irmela Zentner, EDF
Project duration	1 st September 2020 – 31 st August 2024 (48 months)
Related work package	WP4 – Seismic Hazard
Related task(s)	All tasks in WP4
Lead organisation	GEM Foundation
Contributing partner(s)	All the participants to WP4
Due date	2024/04/30
Submission date	2024/07/25
Dissemination level	Public

History

Version	Submitted by	Reviewed by	Date	Comments
N°1.0	M. Pagani	I. Zentner	2024/07/25	



Table of Contents

1.	Introduction	12
1.1.	Procedural Aspects of Probabilistic Seismic Hazard Analysis	12
1.1.1.	IAEA Recommendations	13
1.1.2.	METIS WP4 Objectives	15
2.	WP4 Achievements	15
2.1.	Methodology for Earthquake Catalogue Declustering (D4.1)	15
2.1.1.	Research Motivation	15
2.1.2.	Innovative Aspects of Research Completed	15
2.1.3.	Application of Research and Lesson Learned	16
2.2.	Methodologies for physics-based simulation of ground motion (D4.2 and D4.3) 17	
2.2.1.	Research Motivation	17
2.2.2.	Innovative Aspects of Research Completed	18
2.2.3.	Application of Research and Lesson Learned	18
2.3.	A Bayesian methodology to rank and select Ground Motion Models (D4.6) 21	
2.3.1.	Research Motivation	21
2.3.2.	Innovative Aspects of Research Completed	22
2.3.3.	Application of Research and Lesson Learned	22
2.4.	Computational Aspects of Seismic Hazard Analysis (D4.4)	25
2.4.1.	Research Motivation	25
2.4.2.	Innovative Aspects of Research Completed	25
2.4.3.	Application of Research and Lesson Learned	26
2.5.	Checking and Validation of Probabilistic Seismic Hazard Analysis (D4.5)	27
2.5.1.	Research Motivation	27
2.5.2.	Innovative Aspects of Research Completed	27
2.5.3.	Application of Research and Lesson Learned	28
3.	Conclusions	30
4.	Bibliography	32
5.	Datasets and tools	33
A1.	Conditional Aftershock Probabilistic Analysis for the METIS case study	34



D4.7 PSHA Guidelines

A1.1.	Methodology.....	34
A1.2.	OpenQuake (OQ) Engine Input Model.....	35
A1.3.	Analysis	35
A1.4.	Results	37
A1.5.	Conclusions	39
A1.6.	References	39
A2.	Application of new approach for epistemic uncertainty propagation to the METIS case study.....	40

Figures

- Figure 1 - Illustration of the centre, body, and range of technically defensible interpretations (CBR to TDIs). The centre is the best estimate of the resulting interpretations, the body describes the shape of the distribution about the best estimate, and the range encapsulates the upper and lower limits of the technically defensible interpretations. From: NRC (2018). 13
- Figure 2 - Flow chart showing the IAEA seismic hazard assessment process for nuclear installations. From: IAEA (2022). 14
- Figure 3 - Poisson test score for the METIS case study site undeclustered catalogue (red circle) each investigated declustering algorithm (coloured circles and triangle) well as for two sets of synthetic catalogues with three different number of events (grey triangles). 17
- Figure 4 - Comparison of the attenuation of the spectral accelerations for the RotD50 component (at different frequencies of vibration) of the events populating the SDB, and the recoded reference events. The figure includes also the estimations given by the ESHM20 (Kotha, Weatherill, Bindi, & Cotton, 2020) and the modified Lanzano et al. (2022) ground motion models, here the marker signals the medium and the bars the intervals between the 5th-95th percentiles. 20
- Figure 5 - Simulated pseudo-spectral acceleration (PSA) for the geometric mean of the horizontal components (grey dots) as a function of the Joyner-Boore distance (R_{jb}) for 2 spectral periods ($T=0.01$ s and 2 s) and two magnitudes scenarios ($M_w=5.0$ and $M_w=6.0$). The vertical black bars represent the mean and standard deviation of simulated values over distance bins. Stations within the surface projection of the rupture are plotted at $R_{jb} = 0.1$ km. The GMM for Italy (ITA18) by Lanzano et al. (2019) is plotted in light green (median ± 1 standard deviation) considering a $VS_{30} = 800$ m/s and normal fault mechanism. The median ITA18 adjusted for reference rock conditions according to Lanzano et al. (2022) is shown in red. 21
- Figure 7 - Hazard curves for the METIS test site, considering three scenarios: The mainshock-only hazard curve is shown in blue. The scenario with the aftershock $M_{max} = 7.5$ for all sequences is shown in orange. The scenario with the aftershock $M_{max} = M_{main}$ is shown in green. 27
- Figure 7 - Comparison of the hazard distribution at the France-Germany border in terms of Kolmogorov-Smirnov distance (top) and Wasserstein Distance (bottom). 29
- Figure 9 - Comparison of aggregated seismic hazard curves (blue line for the mean hazard and red dashed lines for the quantiles) and the number of stations exceeding their threshold level according to their set probability and the Binomial distribution with expectation (black line) and 5 – 95 % confidence intervals (grey shaded region). Results are shown for $SA(0.05)$ for the PSHA models ESHM20

- (top row) and Drouet et al., 2020 (bottom row) using ergodic (left columns), partially non-ergodic (centre column, ESHM20 only) and “fully” non-ergodic variability (right).30
- Figure 10 - (left) Mainshock geometry and location for the PGA with return period of 10000 years. (right) Same plot but for the rupture giving the largest contribution to PGA with a return period of 20000 years. The blue dots represent the grid with variable spacing used to distribute the aftershocks around the mainshock rupture.35
- Figure 11 - Density of aftershocks as a function of the closest distance between the centroid of each aftershock rupture and the surface of the mainshock rupture (see Felzer and Brodsky, 2006).....36
- Figure 12 - Aftershock ruptures (in black) and mainshock rupture (red box). The site where we compute the hazard is represented by the red star. (left) Example of simulated aftershock sequence for the rupture giving the largest contribution to PGA with 10000 RP (left) Example of simulated aftershock sequence for the rupture giving the largest contribution to PGA with 20000 RP.37
- Figure 13 - (left) Seismic hazard curves for the conditional aftershock PSHA analysis computed considering as the mainshock the rupture with the largest contribution to PGA with a return period of 10000 years. (right) Seismic hazard curves for the conditional aftershock PSHA analysis computed considering as the mainshock the rupture with the largest contribution to PGA with a return period of 20000 years.37
- Figure 14 - Comparison between the mean hazard computed with the two conditional aftershock PSHA models for the PGA with a RP of 10000 years. The blue curve represents the mean hazard curve computed considering the number and position of ruptures as epistemic uncertainties. The squares in cyan represent the mean hazard curve computed considering the mean model, where these two components of uncertainty are assumed to be aleatory.38
- Figure 15 - Conditional spectrum with a 1% probability of being exceeded in the 30 hours used as the investigation time. The model used to compute this is the mean model of aftershocks generated by the rupture with the largest contribution to the mainshock hazard for PGA with a return period of 1e4 years. The conditioning period is PGA.38
- Figure 16 - Comparison between the mean, 16th and 84th percentile hazard curves for PGA representing the annual frequency of exceedance at the METIS test site as obtained from the OpenQuake Engine with the traditional calculation approach and the with the new approach proposed for the propagation of epistemic uncertainty. In both plots the lower panel shows the comparison between the ratio of the original result over the corresponding one computed using the new approach proposed. [a] Comparison computed considering all the



sources [b] Comparison computed considering only the area source encompassing the site TSZ050.....	41
---	----

Abbreviations and Acronyms

Acronym	Description
GMC	Ground-Motion Characterization
GMM	Ground-Motion Model
GR	Gutenberg-Richter
IAEA	International Atomic Energy Agency
PSA	Pseudo-Spectral Acceleration
PSHA	Probabilistic Seismic Hazard Analysis
SSC	Seismic Source Characterization
SSHAC	Senior Seismic Hazard Analysis Committee



Summary

This deliverable summarises the work done within work package WP4 “Seismic Hazard” of the METIS project and proposes ways to utilise the methodologies put forward within site-specific probabilistic seismic hazard analyses.

The document is organised as follows. The first chapter provide a succinct summary of the key references describing ways to organise a site-specific PSHA project, namely the Senior Seismic Hazard Analysis Committee (SSHAC) Guidelines and International Atomic Energy Agency (IAEA) SSG-9. The former is the reference framework for conducting high-quality site-specific seismic hazard analyses, while the latter provides useful methodological recommendations on how a PSHA analysis must be conducted in order comply with IAEA standards. It is worth to note that within METIS WP4 we focused on methodological components that could be used either to build parts of the seismic hazard input model or to compute results more efficiently, comprehensively, or quickly.

The following chapter contain a description of the main achievements in each of the tasks of WP4. Most of the research within this work package was focused on methodological components (i.e., Tasks from 4.1 until 4.6). Indeed, the METIS Hazard work package (WP4) proposed various improvement to approaches for the computational component of seismic hazard analysis for site-specific applications as well to methods utilized to build parts of a hazard input model.

Within Task 4.1 we developed a new approach for testing and calibrating declustering algorithms which are traditionally used to process earthquake catalogues during the initial stages of the process used to characterise earthquake occurrence, mainly in the case of distributed seismicity sources. The proposed procedure helps to understand the better performing models (i.e. the ones providing a catalogue that contains the largest number of events that can be considered independent) and, possibly, to calibrate them to improve their performance.

A second area where considerable progress was achieved is the one concerning the modelling of ground-motion with physics-based methods. Different research teams tested the applicability of various methods including approaches based on empirical Green’s functions (Irikura’s method and a new one based on spectral decomposition), the 3D simulation approach included in the SCEC broadband platform and the hybrid kinematic stochastic approach as proposed by Otarola et al. in 2016. The latter was used to generate a comprehensive database of synthetic time-histories for the METIS test site. Overall, the methods proposed showed their ability to reproduce observations from events already occurred and provided useful insights on the modelling of ground motion in areas with limited recordings such as the one selected for the METIS case study. These contributions are summarised in Section 2.2.

Still on ground-motion characterisation side, in Section 2.3 we describe an approach based on Bayesian inference trough which it is possible to select ground-motion models from a set of candidate models and to assign weights to each of them. This approach can work with the two main paradigms used for the characterisation of epistemic uncertainty in probabilistic seismic hazard analysis that is the multi-model and the backbone approach.

Regarding the computation of seismic hazard, notable results were obtained with respect to a more comprehensive characterisation of the expected levels of shaking with the implementation of a quite complex and advanced approach for the calculation of the conditional spectrum – as proposed by Lin et al. (2013) – and two novel methods for assessing vector-valued PSHA. About the modelling of epistemic uncertainty, we proposed a new approach that for a given site combines more efficiently the realizations admitted by single-source logic-trees modelling epistemic uncertainties for the sources of engineering importance for the investigated site. These methodological improvements offer new perspectives for a more comprehensive modelling of seismic hazard for nuclear installations. Finally, to explore the impact of accounting for the contribution of aftershocks into the modelling of risk for nuclear power plants, we developed two approaches for computing aftershock seismic hazard. The first one follows the approach put



forward by Boyd (2012) and has the advantage of starting from a conventional probabilistic seismic hazard input model based on main shocks. The second approach – more specifically tailored to the need of METIS and more in general of risk-assessment studies for nuclear installations – computes conditional seismic hazard, starting from the occurrence of a mainshock.

The last noteworthy contribution of the METIS project to hazard modelling is an original approach to quantitatively compare the results of alternative seismic hazard models for a region, as well as assess whether the PSHA model estimates are consistent with observed ground motions. To facilitate the use of these approaches, an ad-hoc software package called PyPSHATest was created in WP4.5. PyPSHATest is an open-source Python toolkit for quantitative model-to-model and model-to-observation comparison probabilistic seismic hazard results.

Keywords

Probabilistic Seismic Hazard Analysis, Seismic Source Characterisation, Ground-Motion Characterisation



1. Introduction

1.1. Procedural Aspects of Probabilistic Seismic Hazard Analysis

A key prerequisite to seismic probabilistic safety assessment for nuclear installations is the analysis of the seismic hazard at the site. Probabilistic Seismic Hazard Analysis (PSHA) is widely used as standard practice to assess the seismic hazard at the site of a nuclear installation.

First, the seismic source characterisation (SSC) component of a PSHA model describes the spatial and temporal distribution of earthquakes on all local seismic sources of relevance to the site of interest. Specifically, probability models are utilised to estimate the spatial location of potential future earthquakes, the geometry and characteristics of such earthquake ruptures, the frequency and size distribution of these earthquakes, and maximum magnitude earthquake to be considered in the analysis. Next, the ground-motion characterization (GMC) component of PSHA uses a suite of semiempirical ground-motion models (GMMs) selected to estimate the ground shaking intensity of each rupture scenario given the magnitude, distance, and other predictor variables. The SSC and GMC are then combined to calculate the expected rates of exceedances for different ground-motion levels for the site, which are called hazard curves.

In performing a PSHA, uncertainties in the state of knowledge about earthquake processes are explicitly accounted for. First, aleatory variability, which refers to random outcomes resulting from the inherent variability in a natural process for a particular model formulation of that process, is modelled by a probability distribution in the PSHA model and controls the shape of this hazard. Second, epistemic uncertainty, which refers to the lack of knowledge due to limitations in observed data, or limitations in our understanding of the physics underlying the process. This epistemic uncertainty is considered using logic trees to incorporate multiple assumptions, hypotheses, models, or parameter values. Each realization of the overall logic tree corresponds to an interpretation of the state of nature and results in a hazard curve. These weighted hazard curves lead to a statistical distribution of hazard estimates for the site.

In METIS WP4, we did not focus on procedural aspects of PSHA since there is extensive literature on this subject largely endorsed by the scientific and technical communities. We provide, for reference, a concise description of the SSHAC process and IAEA SSG-9 guidelines. It is also worth noting that, given the constraints in the project, we did not manage to follow the SSHAC process while implementing the hazard model for the METIS case study. SSHAC Guidelines

The United States (U.S.) Nuclear Regulatory Commission (NRC) provides guidance for conducting earthquake hazard assessments through the structured, transparent framework that is referred to as the Senior Seismic Hazard Analysis Committee (SSHAC) process. The original SSHAC guidance provided in NUREG/CR-6372, "Recommendation for Probabilistic Seismic Hazard Analysis: Guidance on Uncertainty and the Use of Experts" (NRC, 1997), are strengthened, clarified, and built upon by NUREG-2213, "Updated Implementation Guidelines for SSHAC Hazard Studies" (NRC, 2018). The SSHAC guidelines define four levels at which seismic hazard assessment studies can be conducted, which increase in complexity, confidence, and cost from Level 1 through Level 4. The four levels share the same basic attributes but differ in implementation. The NRC guidance and the SSHAC approach are not limited to applications within the United States but are employed internationally to satisfy the need for regulatory assurance within a range of regulatory environments for both nuclear and non-nuclear critical facilities (e.g., Bommer et al., 2015).

There are five fundamental features required for all four levels of SSHAC studies:

1. Clearly defined roles and responsibilities of all participants.

2. Objective evaluation of all available data, models, and methods that could be relevant to the characterization of the hazard at the site, including the limits, gaps, and the resolution and uncertainties in the available existing data.
3. The hazard input models for seismic source characterization (SSC) and ground motion characterization (GMC) will address both aleatory variability and epistemic uncertainties, to represent the centre, body, and range of technically defensible interpretations (CBR of TDIs; Figure 1).
4. Documentation will be complete and transparent to justify in sufficient detail the technical interpretations that support the hazard input models and allow the hazard analyses to be reproduced by an external reviewer.
5. Independent participatory peer review to confirm that the evaluation was conducted objectively and without cognitive bias and that the requirements of the previous four points have been met.

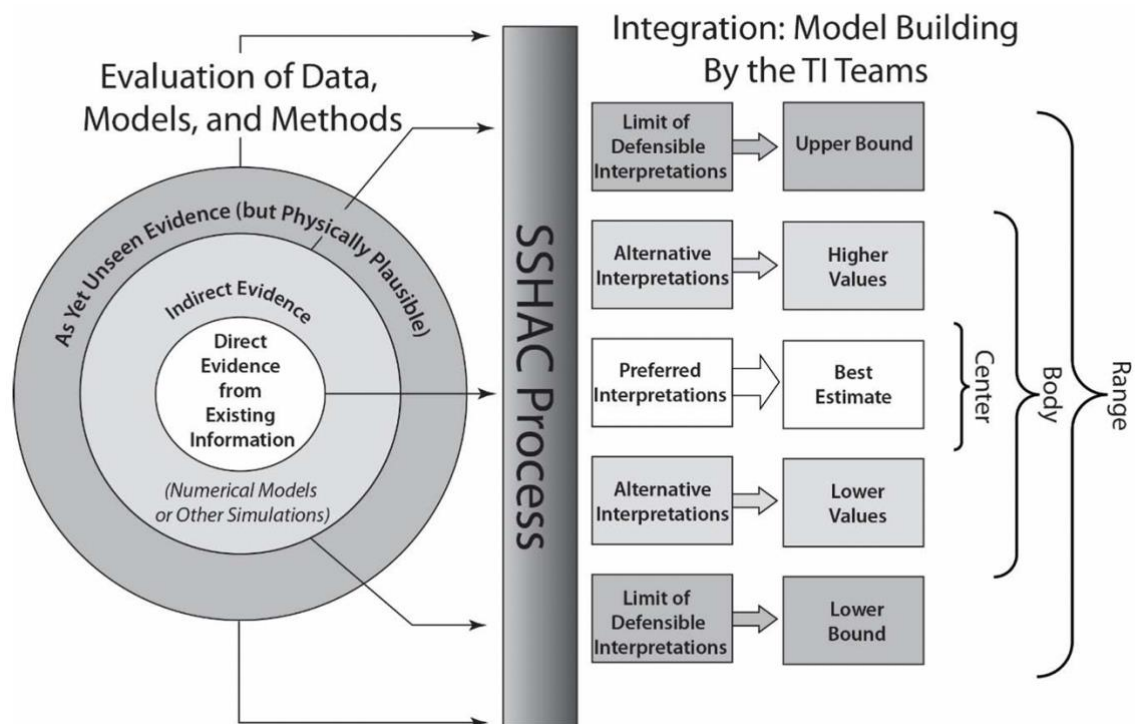


Figure 1 - Illustration of the centre, body, and range of technically defensible interpretations (CBR to TDIs). The centre is the best estimate of the resulting interpretations, the body describes the shape of the distribution about the best estimate, and the range encapsulates the upper and lower limits of the technically defensible interpretations. From: NRC (2018).

1.1.1. IAEA Recommendations

The International Atomic Energy Agency (IAEA) Safety Standards Series No. SSG-9 (Rev. 1), Seismic Hazards in Site Evaluation for Nuclear Installations, provides the latest IAEA recommendations on how to meet requirements relating to the evaluation of earthquake hazards that might affect nuclear installations. This IAEA safety guide is intended for use in any seismotectonic environment by not only the regulatory bodies responsible for establishing regulatory requirements but also by the operating organizations of the nuclear installation. Then, recommendations for the determination of the appropriate basis for the design and evaluation of a nuclear installation through the use and application of appropriate criteria are provided in IAEA Safety Standards Series No. SSG-67, Seismic Design for Nuclear Installations.

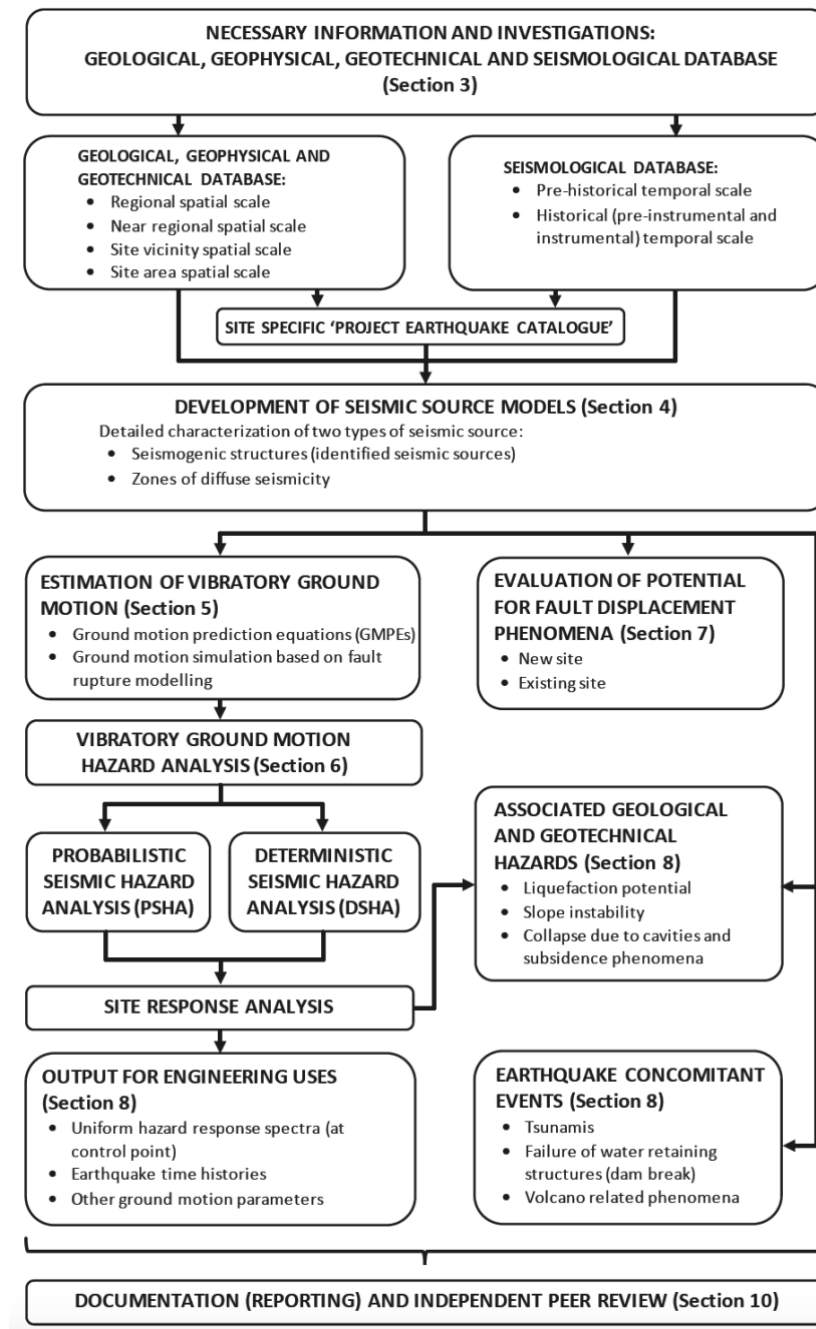


Figure 2 - Flow chart showing the IAEA seismic hazard assessment process for nuclear installations. From: IAEA (2022).

Safety guide SSG-9 (Rev. 1) provides recommendations for the compilation a comprehensive and integrated database of geological, geophysical, geotechnical, and seismological information, as well as the integration of the information in this database into a seismic source model. There are also recommendations for the evaluation of ground motion from potential future earthquakes and the probabilistic and/or deterministic methods of seismic hazard analysis for the nuclear installation, and the necessary outputs of this hazard analysis for engineering uses. There are also sections on fault displacement hazard, as well as earthquake associated hazards such as liquefaction, slope instability, and subsidence (Figure 2).

1.1.2. METIS WP4 Objectives

WP4 of the METIS Project aims to develop new approaches and tools to improve the current state of practice for the calculation of seismic hazard. The WP4 activities comprise seven work tasks covering different components of the seismic hazard analysis process: the characterisation of earthquake occurrence, the calculation of ground-motion, the definition of epistemic uncertainty, the calculation of seismic hazard (with probabilistic and physics-based approaches), the checking of hazard results and the application of these methodologies to the METIS case study.

In the context of the METIS project, it was deemed important to demonstrate the application of the newly developed methods and tools to a case study nuclear installation. The METIS case study site is a hybrid site in which a hypothetical Zaporizhzhia Nuclear Power Plant (ZNPP)-like nuclear installation exists on the western coast of Tuscany, Italy. Due to the lack of an existing site-specific seismic hazard study for the METIS hybrid site, a relatively simple seismic hazard model was produced to test and apply the various methods and tools developed in the METIS project.

In this, the final deliverable of WP4, we provide an overview of the new PSHA tools and methods developed in this work package and the innovations made to current practice.

2. WP4 Achievements

2.1. Methodology for Earthquake Catalogue Declustering (D4.1)

2.1.1. Research Motivation

A fundamental dataset in the construction of a SSC is an earthquake catalogue of historical (instrumental and/or pre-instrumental) earthquake events in the region of interest. However, a necessary assumption in time independent PSHA is that earthquake occurrence can be represented by a stationary Poisson process, i.e., earthquakes events are independent. Yet earthquake catalogues inherently contain earthquake events that cluster in space and time, e.g., foreshocks and aftershocks. Therefore, to only consider independent earthquake events in the SSC, dependent events in the catalogue needs to be identified and removed, which is commonly conducted using declustering algorithms.

Conventional methods of earthquake catalogue declustering involve removing all events that occur within a given space-time magnitude-dependent window around another earthquake (Gardner and Knopoff, 1974). However, while these declustered catalogues are more Poissonian and so have more stable earthquake rates, the holes (space-time domains with no earthquakes) created by the removal of a larger number of smaller magnitude earthquake from the catalogue may not only artificially modify the resulting magnitude-frequency distribution but also may lead to an underestimation of the seismic hazard and risk (Gerstenberger et al., 2020). Therefore, there is a need during the development of a SSC to carefully consider and balance these trade-offs and have declustering algorithms developed that produce the 'best' balance.

2.1.2. Innovative Aspects of Research Completed

To address this need, in WP4.1 of the METIS project (Chartier and Pagani, 2022) a new method was developed to test and quantify the Poissonian nature of an earthquake catalogue, to compare the performance of alternative declustering algorithms. The availability of this information can allow an informed decision to be made about the relative balance between the number of earthquakes retained by a given declustering algorithm and the Poisson nature of the resulting declustered catalogue. This, in turn, then can inform the declustering algorithm(s) to be selected for the SSC. This innovative Poisson testing method considers whether the temporal and spatial distribution of the seismicity in a declustered catalogue has statistical

properties like that of a synthetic Poisson catalogue (that has the same temporal and spatial distribution and contains the same number of earthquakes). Specifically, this new method is based on the calculation of the inter-earthquake spatiotemporal distances between each event in a given catalogue, which is described as a probability mass density function for the catalogue. A strongly clustered catalogue will have more similar inter-earthquake spatiotemporal distances than a synthetic Poisson catalogue. This difference is used to calculate a Poisson test score for a catalogue between 0 and 1, where a higher value indicates a more Poisson nature.

The Poisson test score of a declustered catalogue can then be considered in combination with the number of events retained within the catalogue to make a balanced decision about the relative merit of a given declustering algorithm. Importantly, the relative Poisson test scores of alternative declustering algorithms provides an objective method for not only selecting the declustering algorithms to be used for a study SSC logic tree, but also for assigning the relative weights of logic tree branches at a potential declustering logic tree node. The result is a better constrained magnitude-frequency distribution, due to the increased number of retained events, that is not at risk of erroneously over-estimating the hazard, due to the declustered catalogue receiving a high Poisson test score.

In addition, a new declustering algorithm was developed during WP4.1 utilising the inter-earthquake spatiotemporal distance method established for the Poisson test score. For this new declustering algorithm, two events in an earthquake catalogue are part of a cluster if the calculated inter-earthquake spatiotemporal distance is below a critical distance. This new declustering algorithm is referred to as t411. An advantage of this new declustering algorithm t411 is that it is readily combined with the catalogue Poisson test, which allows the investigation and selection of the critical distance that optimises the number of events retained and the Poisson test score.

2.1.3. Application of Research and Lesson Learned

This newly developed catalogue Poisson test method was applied to investigate the performance of different declustering algorithms for an earthquake catalogue of relevance the METIS case study site in Central Italy. Five established declustering algorithms, including both window and nearest neighbour approaches, as well as the new t411 declustering algorithm were applied to the ISC bulletin catalogue of $M_w \geq 3.5$ earthquake events between the years 1960 and 2020. These inter-earthquake spatiotemporal distances of each declustered catalogue were compared to a synthetic Poisson catalogue generated for the region, and Poisson test scores were determined for each declustered catalogue (Figure 3).

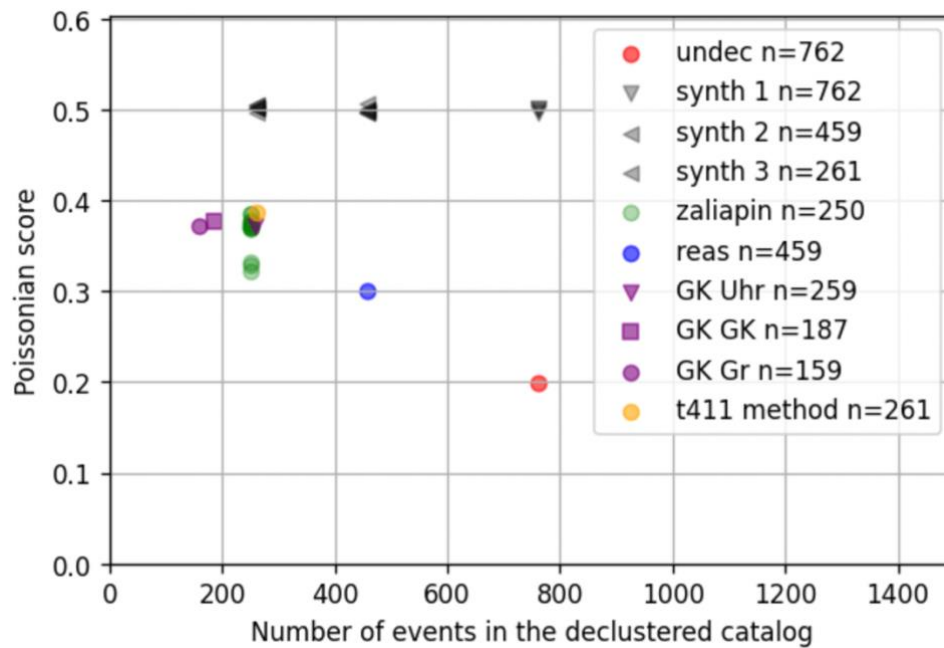


Figure 3 - Poisson test score for the METIS case study site undeclustered catalogue (red circle) each investigated declustering algorithm (coloured circles and triangle) well as for two sets of synthetic catalogues with three different number of events (grey triangles).

Finally, to demonstrate the benefit to PSHA from the information gained by the catalogue Poisson test score, each of the six declustered catalogues were developed into a PSHA model SSC. The ESHM20 area source geometries were used, and the hazard estimates were calculated for the METIS case study site as well as a higher seismicity site in the Central Apennines. The results revealed that impact of the declustering approach on the hazard results is greater for the site located in the more seismically active region, closer to many earthquake clusters, than for the site in the stable region where the declustering removes only few earthquakes. Therefore, the Poisson test score method developed during this METIS work package is most valuable when assessing the hazard of areas with higher past seismicity. Nonetheless, this methodology was applied for the construction of the seismic source characterization for the METIS case study (see METIS Deliverable 4.6; see Pagani et al., 2023).

2.2. Methodologies for physics-based simulation of ground motion (D4.2 and D4.3)

2.2.1. Research Motivation

The estimation of earthquake ground motions at reference bedrock conditions is a necessary component of seismic risk assessment because the target site is located on outcropping bedrock, or because soil response will be subsequently integrated by soil response analysis. However, many strong-motion databases contain earthquake recordings of stations installed on soil or soft-rock sites, with very few stations on hard-rock sites. Moreover, the definition of reference rock may vary from one application to the next and site conditions, not to mention that site conditions are not always thoroughly documented in databases of recorded ground motions. Additionally, for nuclear safety assessment it is necessary to consider very long return periods, for which the large ground-motion intensities have not been instrumentally recorded. This limitation in available records may be overcome by the simulation of rock ground motion or by correcting observed ground motion from site effects.

2.2.2. Innovative Aspects of Research Completed

In METIS WP4.5 (Zentner et al., 2024), ground motion simulation methods were introduced and contrasted with the intention to generate synthetic ground motion time histories on bedrock using source and path terms consistent with the ones used to compute seismic hazard. Specifically, a suite of open-source tools to perform physics-based simulations, including stochastic, empirical and hybrid models, for engineering application were compared.

The following approaches were analysed alongside with the validations presented by their authors:

- i. The Irikura recipe with empirical Green's functions (EGF). This is an approach applied worldwide to simulate large crustal earthquakes and is widely used in Japan for seismic safety evaluations of nuclear power plants (IAEA 2015). Here, the use of this approach was validated using the 2007 Mw 6.6 Chuetsu-oki earthquake and the strong ground motions recorded at the Kashiwazaki-Kariwa Nuclear Power Plant (KK NPP) site.
- ii. A 3-D stochastic physics-based approach using Southern California Earthquake Center (SCEC) Broadband Platform (BBP) and tailored for Europe. Here, this approach was first validated by the comparison of the simulated ground motions with the recorded and empirical GMM of the 2016 Mw 6.2 Amatrice earthquake of Central Italy. Second, the consistency of the variability (standard deviation) of the simulations with empirical GMM estimates using a database with simulated ground motion time histories based on a stochastic catalogue of ruptures for the Rhine Graben area.
- iii. A stochastic ground motion simulation approach based on an enhanced Otarola method. Here, this approach was validated by comparing the simulations with the GMMs for Japanese scenario earthquakes and comparison the engineering demand parameter for Europe.
- iv. Recorded ground motions corrected for site term. This approach applies a physics-based correction to remove site effects from surface recordings to obtain the underlying bedrock motion. This approach was validated against recordings at downhole sensors at KiK-net sites.
- v. The combination of spectral decomposition of ground motion with EGF simulation techniques to simulate region-specific reference bedrock time histories. This method is referred to in D4.3 as the "Seister approach". This approach was validated based on a large set of earthquakes recordings in Central Italy (Ameri et al., 2024)

2.2.3. Application of Research and Lesson Learned

The third and fifth investigated approaches, the enhanced Otarola and Seister approach, respectively, were selected as the preferred approaches and applied to the METIS case study site, where the moderate seismicity of the region is characterized by a limited number of data and available rock motions.

The enhanced Otarola method was originally presented by Otarola et al., (2016) and Ruiz et al., (2019), and later modified by Alvarez (2022). This ground motion simulation technique builds over other stochastic methods such as those presented in Boore (1983), Boore and Atkinson (1997) and Motazedian et al., (2005), by incorporating a model for the full body wave field spectra (i.e., P, SV and SH-waves). Another advantage of this technique is the physical meaning of the parameters used in the construction of the synthetic ground motions, this feature allows a direct link between seismicity recorded at the region and subsequent simulations, using source and path terms consistent with the ones used to compute seismic hazard. Applications such as that presented deliverable DP5.1 have demonstrated the compatibility of the technique for the generation of databases of simulated ground motions to be used for earthquake response assessment.

To generate the database of simulated ground motions for the METIS case study a series of steps were followed. First, a set of input parameters (for a similar model) was obtained from the literature for the region of interest. Next, a set of ground motions recorded in the region of



interest was selected for its use as reference in the calibration of these input parameters to accommodate the differences with the enhanced Otarola method. Finally, the calibrated model was used to generate a database of simulated ground motions, populated with new earthquake scenarios consistent with those obtained from the disaggregation of the hazard computed for the METIS case study. Figure 5 shows a comparison of the spectral accelerations at different frequencies for simulated and recorded scenarios, and the ground motion models considered in the PSHA of the METIS case study.

In the Seister approach, first, the nonparametric spectral decomposition approach (also called the generalized inversion technique, GIT) was applied to separate the contribution of source, path, and site from the observed Fourier spectra of a dataset of recordings covering central Italy. The average source and site effects are removed from observed small-magnitude recordings in the target region through deconvolution in the Fourier domain. This way, the obtained deconvolved signals represent path term only (effectively EGFs). Then, we couple the EGFs with k-2 kinematic rupture models for target scenario events. For each target magnitude, a set of rupture models following a ω -squared source spectrum are generated sampling the uncertainties in kinematic source parameters. The proposed approach is validated using recorded ground motions at reference sites from multiple earthquakes in Central Italy (Ameri et al. 2024). The power of this approach lies in its ability to map the path-specific effects into the ground-motion field, providing 3-component time histories covering a wide frequency range, without the need for computationally expensive approaches. The simulated spectral accelerations from the synthetic time histories were compared to the empirical Lanzano et al. 2019 and 2022 GMMs for Italy. Figure 5 shows the consistency of the simulated values with the Italian GMM ground-motion estimates.

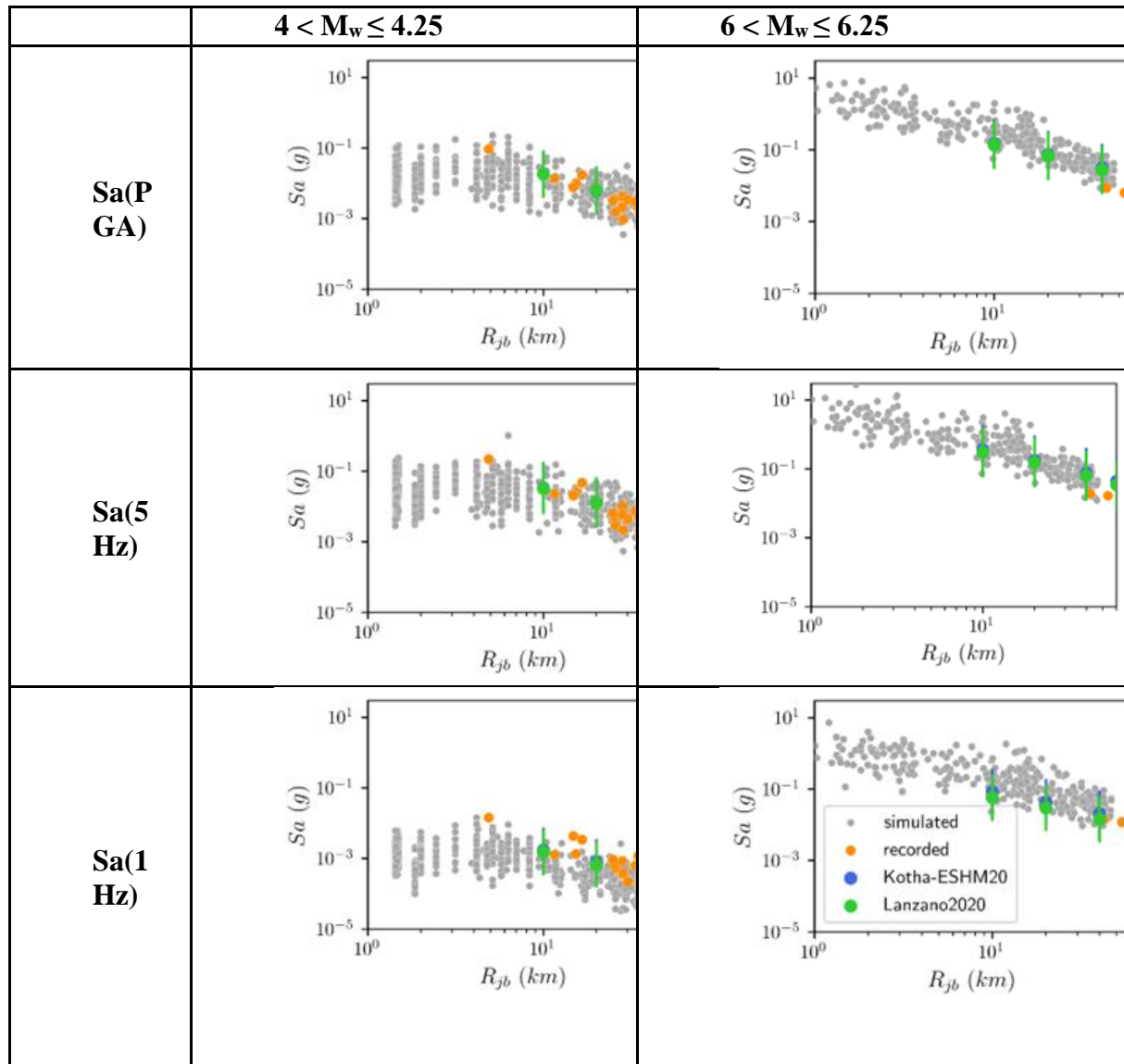


Figure 4 - Comparison of the attenuation of the spectral accelerations for the RotD50 component (at different frequencies of vibration) of the events populating the SDB, and the recoded reference events. The figure includes also the estimations given by the ESHM20 (Kotha, Weatherill, Bindi, & Cotton, 2020) and the modified Lanzano et al. (2022) ground motion models, here the marker signals the medium and the bars the intervals between the 5th-95th percentiles.

Importantly, this METIS activity builds on work conducted in WP5, which can be found in deliverable D5.1, "Methodology for selecting ensembles of rock-hazard consistent ground motions for fragility curve computations and datasets for WP6". In D5.1, more detail can be found on the ground motion selection strategies developed within METIS, alongside the engineering validation of stochastic ground motion databases generated with the ground motion simulation methodology.

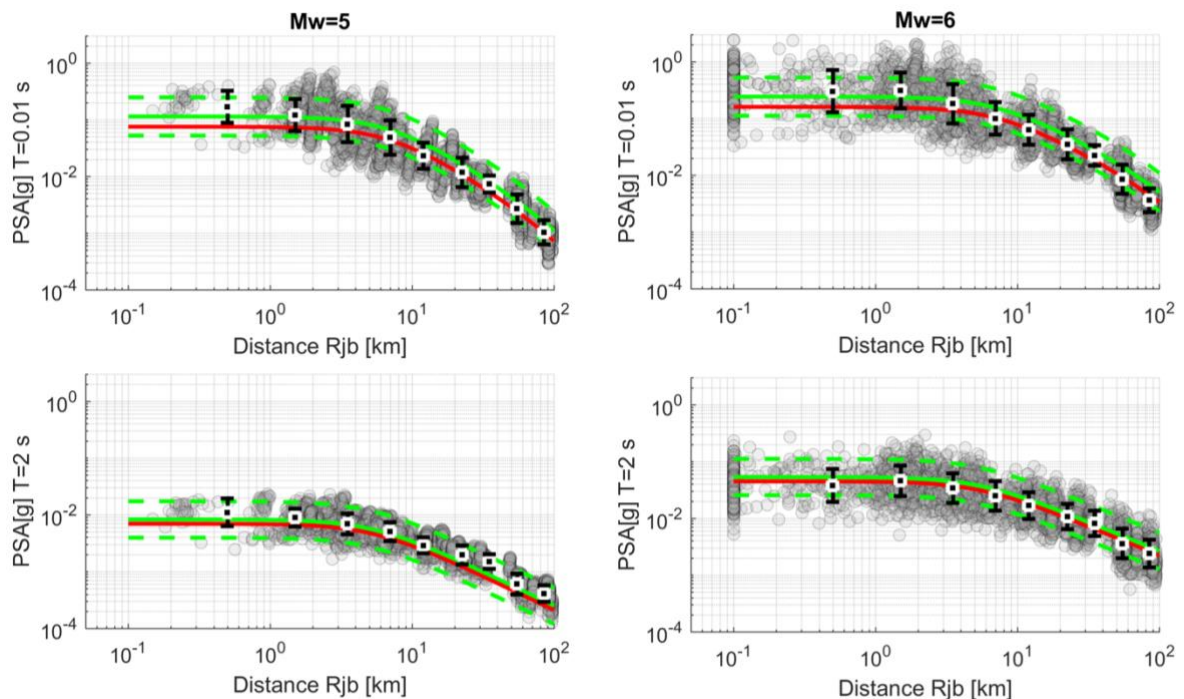


Figure 5 - Simulated pseudo-spectral acceleration (PSA) for the geometric mean of the horizontal components (grey dots) as a function of the Joyner-Boore distance (R_{jb}) for 2 spectral periods ($T=0.01$ s and 2 s) and two magnitudes scenarios ($M_w=5.0$ and $M_w=6.0$). The vertical black bars represent the mean and standard deviation of simulated values over distance bins. Stations within the surface projection of the rupture are plotted at $R_{jb} = 0.1$ km. The GMM for Italy (ITA18) by Lanzano et al. (2019) is plotted in light green (median ± 1 standard deviation) considering a $VS_{30} = 800$ m/s and normal fault mechanism. The median ITA18 adjusted for reference rock conditions according to Lanzano et al. (2022) is shown in red.

2.3. A Bayesian methodology to rank and select Ground Motion Models (D4.6)

The research described in this section was not applied to the METIS case study. Nonetheless, we keep it in this report since it still represents one important contribution to WP4 provided by one of the associated organisations.

2.3.1. Research Motivation

Recent studies have shown that significant uncertainties exist in the evaluation of the seismic hazard, especially in the regions with low-to-moderate seismicity, due to the scarcity of recorded earthquake data and lack of precise knowledge concerning the earthquake generation and propagation mechanisms. The epistemic uncertainty in ground motion models (GMMs) is accounted for using a conventional logic tree approach. In the last decade, the use of a backbone approach to account for epistemic uncertainty has gained significant attention. Both logic tree and backbone approaches involve ranking or selection of GMMs from a list of candidate GMMs. In standard practices, the estimate of branch or model weights in a logic tree is based on expert judgment and there is no holistic approach for ranking the GMMs under uncertainty. Similarly, there is no one standard method for selecting the best GMM as the backbone model. Therefore, in this research, we propose a statistical methodology that is based on Bayesian inference, to rank and select the GMMs from a list of candidate GMMs.

2.3.2. Innovative Aspects of Research Completed

The main objective of this research is to provide quantitatively based recommendations to the experts so that they can make a more informed judgment. In this study, we employ the Bayesian model averaging (BMA) methodology to rank and select the GMMs from a list of candidate GMMs. Bayesian linear models (BLM) are used as an estimation method to calculate the model evidence of the candidate GMMs without any approximations, and subsequently, GMMs are ranked and weighted. The proposed methodology can assist experts to make a better judgment by going from a heuristic approach to a quantified or semi-quantified approach.

The conventional logic tree approach still requires some degree of subjectivity where the experts can assign branch weights based on the model evidence or marginal likelihood. Candidate GMMs with relatively very less model evidence can be ignored and thereby the number of branches in a logic tree can be reduced.

BMA approach integrates model uncertainty by averaging the predictions of overall candidate GMMs. The BMA model has a lower mean squared error than any of the GMMs at all periods for the testing data set indicating that the BMA model yields the most optimal predictions.

2.3.3. Application of Research and Lesson Learned

In this research, five GMMs are selected, and OpenQuake Engine library is used to test their performance against ESM database. Then, a smaller subset of the ESM database with 231 observations is considered based on the following selection criteria: moment magnitude [4; 5], epicentral distance [4; 150 km], velocity [800; 1200 m/s], and reverse fault mechanism. The data set is divided into training (70%) and testing (30%) data sets randomly.

The marginal likelihood of all candidate GMMs is evaluated at all periods using BLM approach. Table 1 shows the ranking and weights of GMMs at different time periods. As seen in Table 1, no single GMM dominates over the entire range of periods. The weights can be used in a conventional logic tree approach to propagate epistemic uncertainty or the GMMs with the highest rank can be chosen as the backbone model in a backbone approach. At $T = 0.1$ s, Bindi et al. (2011) completely takes over ($w \approx 1$) the other GMMs indicating that the BMA approach boils down to model selection.

Table 1. Model evidence of candidate GMMs

Period	Measure	Bindi2011	Akkar2014	Bindi2014	Boore2014	Cauzzi2015
PGA	ML	-520.36	-524.36	-528.17	-528.94	-528.47
	Rank	1	2	3	5	4
	Weight	0.98132	0.01781	0.00039	0.00018	0.00029
0.1 sec	ML	-532.62	-537.35	-539.83	-543.56	-541.98
	Rank	1	2	3	5	4
	Weight	0.99044	0.00873	0.00073	2e-05	8e-05
0.2 sec	ML	-526.95	-528.09	-533.5	-534.57	-534.54
	Rank	1	2	3	5	4
	Weight	0.75511	0.24305	0.00109	0.00037	0.00038
0.3 sec	ML	-523.21	-523.17	-528.5	-527.97	-527.82
	Rank	2	1	5	4	3

	Weight	0.48642	0.50215	0.00244	0.00415	0.00484
0.4 sec	ML	-514.87	-513.52	-519.48	-517.79	-517.12
	Rank	2	1	5	4	3
	Weight	0.19963	0.76669	0.00198	0.01073	0.02097
0.5 sec	ML	-509.11	-506.52	-512.4	-510.6	-509.56
	Rank	2	1	5	4	3
	Weight	0.0658	0.8747	0.00245	0.01484	0.0422
0.6 sec	ML	-509.76	-506.85	-513.24	-511.03	-509.13
	Rank	3	1	5	4	2
	Weight	0.04644	0.85175	0.00144	0.01306	0.08732
0.7 sec	ML	-506.59	-502.68	-508.93	-505.95	-503.37
	Rank	4	1	5	3	2
	Weight	0.01282	0.64172	0.00124	0.02427	0.31996
0.8 sec	ML	-507.03	-503.42	-508.13	-505.71	-503.07
	Rank	4	2	5	3	1
	Weight	0.01053	0.3915	0.00352	0.03968	0.55477
0.9 sec	ML	-505.64	-501.88	-505.77	-503.28	-501.58
	Rank	4	2	5	3	1
	Weight	0.00877	0.37908	0.00772	0.09304	0.51139
1 sec	ML	-505.24	-500.76	-503.89	-501.77	-500.14
	Rank	5	2	4	3	1
	Weight	0.00346	0.30543	0.01331	0.11157	0.56623

After obtaining the ranks and weights of different GMMs, the ESM testing data set is used for testing the efficiency of the candidate GMMs. The posterior predictive distribution of the GMMs with added bias term is obtained and the BMA predictions are computed. The mean squared error (MSE) is employed as a performance metric. Figure 9 shows the performance of all candidate GMMs and the BMA model against the testing data set. As seen in Figure 9, the BMA model has the lowest MSE compared to other GMMs at all periods. Therefore, the BMA model can be used as the backbone model in a backbone approach.

While we certainly recognize the relevance of this approach for site-specific hazard analysis, for the selection of ground models used for the calculation of hazard for the METIS case study (Pagani et al., 2023) we opted for a simpler characterization based on the most recent ground-motion models available for the Italian context. This choice was dictated by the need to keep the structure of the hazard input model simple and - therefore - suitable for testing other methodologies developed within the METIS project.

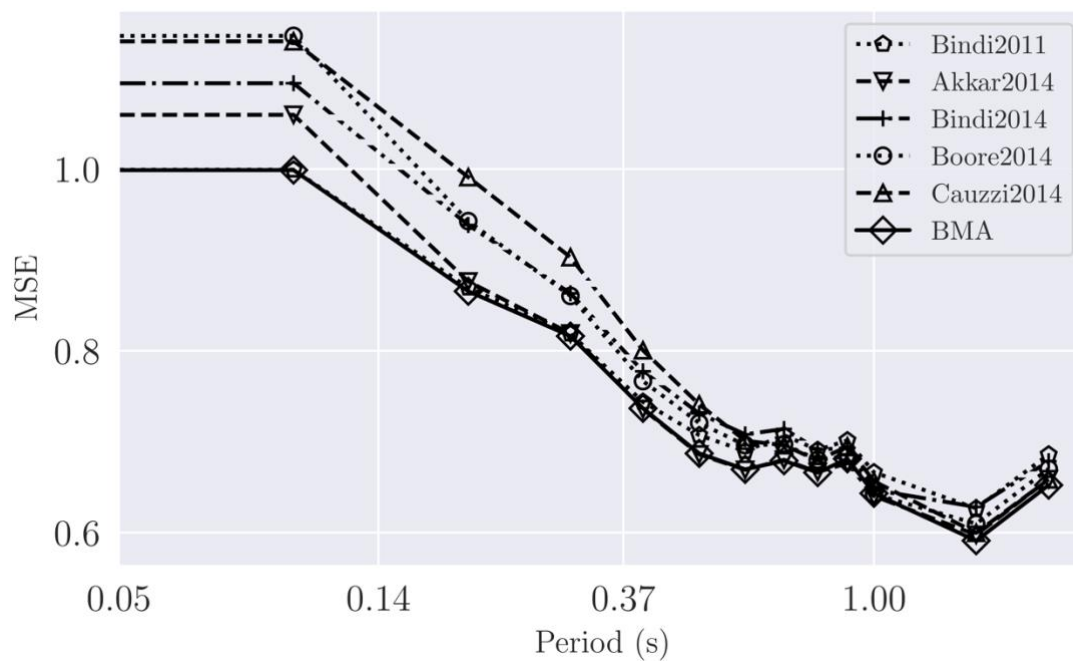


Figure 9 - Performance of GMMs and BMA model against testing data set



2.4. Computational Aspects of Seismic Hazard Analysis (D4.4)

2.4.1. Research Motivation

Deliverable 4.4. summarises the main results achieved in METIS regarding the methodological improvements to PSHA (Pagani et al., 2024).

During the development of PSHA models for nuclear installations there is great importance placed on capturing the full spectrum of epistemic uncertainties, to sufficiently represent the centre, body, and range of technically defensible interpretations. However, it is often not computationally feasible to calculate hazard estimates for the millions of individual realisations of the complex, resultant logic tree. Therefore, sampling of this complete logic tree becomes necessary to instead calculate hazard estimates for only a subset of the realisations. To improve computational aspects of PSHA, a first task is focused on the propagation and computation of epistemic uncertainties.

Vector-valued PSHA (VPSHA), which describes the mean rate of occurrence (or exceedance) of multiple intensity measure types, provides a more comprehensive description of ground motion for seismic risk analyses than scalar PSHA. However, despite the advantages, VPSHA is rarely used in common practice. Additionally, ground motion selection for structural analysis is often associated with a conditional spectrum (CS) that estimates the distribution (with mean and standard deviation) of the response spectrum, conditioned on the occurrence of a target spectral acceleration value at the period of interest. However, multiple earthquake scenarios contribute to the occurrence of a given ground motion intensity and PSHA models utilise a logic tree of multiple SSC and GMC models, which need to be incorporated to compute a CS that is fully consistent with the PSHA calculations upon which it is based. To improve computational aspects of PSHA, a second task is focused on implementing computationally efficient methods of both VPSHA and CS calculations.

Aftershocks are not typically considered in regional, long-term PSHA. However, the impact of aftershocks becomes greatly important when considering the seismic safety assessment of systems, structures, and components of nuclear installations. Epidemic-Type Aftershock Sequences (ETAS) approaches generate a long synthetic catalogue of aftershock sequences for each mainshock. However, using the ETAS approach, each of these stochastic events need to be long enough to evaluate the rare ruptures over the long return periods of relevance to nuclear installations. To improve computational aspects of PSHA, a third task is focused on incorporating aftershocks into classical PSHA in a more computationally efficient manner.

2.4.2. Innovative Aspects of Research Completed

The first task, 'Approaches for the Propagation of Epistemic Uncertainty', improved the processing of logic tree epistemic uncertainties in PSHA. First, the option of using a Latin Hypercube sampling approach, as opposed to a conventional Monte Carlo approach, was incorporated as an option to the hazard modeller and, second, the decision was added to apply the weights to the logic tree before or after the sampling. Of great significance, is that a new approach was developed that computes seismic hazard for each individual source-specific logic tree and combines the results using discrete distributions via a convolution approach. Importantly, correlated uncertainties, such as when multiple sources belong to the same tectonic region type or when two fault sources share the same variability of the seismogenic thickness, are explicitly accounted for by splitting the sources into groups, where each group contains the sources sharing correlated epistemic uncertainties. This new method for propagating epistemic uncertainties not only provides results that are consistent with those using traditional approaches but also the calculation of the results is more computationally efficient.

The second task, 'Vector-valued PSHA and CS Approach', developed a new approach to calculate vector-valued PSHA and implemented the most complete, rigorous, and complex calculation approach currently available for the calculation of the conditional spectrum. First,



the developed VPSHA methodology applies the 'indirect' approach of performing a disaggregation to compute the mean rate density. Whereas normally the calculation efficiency is greatly reduced by the large multidimensional matrix required to store the disaggregation results required to exhaustively consider the GMM explanatory variables, here a four dimensional 'kernel' matrix is used to store the rates of occurrence of discrete combinations of the median values and corresponding standard deviations of the two intensity measure types selected. Importantly, this approach is implemented as a post-processing tool that reuses the results of a previous classical PSHA for the same site and set of IMTs. Second, the most complex CS approach of Lin et al (2013), 'Method 4', was implemented, which integrates the contributions from the ruptures in all the realizations admitted by the hazard model logic tree.

The third task, "Modelling earthquake sequences for considering aftershocks", developed tools for adjusting the rates of mainshock models to account for the contribution of aftershocks. A new approach, of incorporating aftershocks directly into a classical PSHA was developed by identifying the time-independent rate that each rupture would occur as an aftershock of each mainshock rupture in the source model. The developed method assumes that all the aftershocks occur on existing ruptures within the seismic source model, therefore, any existing seismic hazard model is suitable for classical PSHA with aftershocks considered as well. Additionally, the methods developed here for Classical PSHA with Aftershocks may be easily modified or extended to support the creation of stochastic event sets for single mainshock-aftershock sequences or for model-wide sequences.

Vector valued PSHA using the copula approach

The approach for vector PSHA implemented in the OpenQuake Engine software allows for the computation of multidimensional hazard curves without simplifying assumptions from former approaches but it is computationally very demanding and cannot be run on a PC. This is why, in addition, we have implemented a handy yet rigorous approach that allows for obtaining vector hazard by means of the copula approach. This approach only requires the common scalar hazard curves and the correlation coefficient to compute vector hazard in a post-processing procedure.

2.4.3. Application of Research and Lesson Learned

The PSHA code selected for performing hazard calculations for the METIS project is the OpenQuake Engine (Pagani et al., 2014), developed by the Global Earthquake Model (GEM) Foundation. Therefore, the capabilities of the OpenQuake engine were expanded as the approaches and tools developed during WP4 were incorporated. For that reason, these new approaches and tools developed during the METIS project are freely available to be implemented in future PSHA models developed using the OpenQuake Engine.

For the METIS case study site, the methods developed in the third task for the consideration of aftershocks were applied to the hazard model for the site, and the impact on the hazard results of incorporating aftershocks into the PSHA model was investigated. The hazard curves for the METIS case study site (Figure 6) show the substantial increase in seismic hazard when aftershocks are considered, compared to conventional PSHA without the consideration of aftershocks. The amount of increase varies with the return period of interest and the maximum magnitude of the aftershock.

Within the work packages 6 and 7 of the METIS projects, it has been decided that to account for the contribution of aftershocks while performing the Probabilistic Safety Analyses (PSA) of nuclear power plants, it is more appropriate to compute the conditional hazard produced by the aftershock sequence triggered by a mainshock. To provide results compatible with this requirement we developed an ad-hoc methodology that it is described in Appendix A1 of this document.

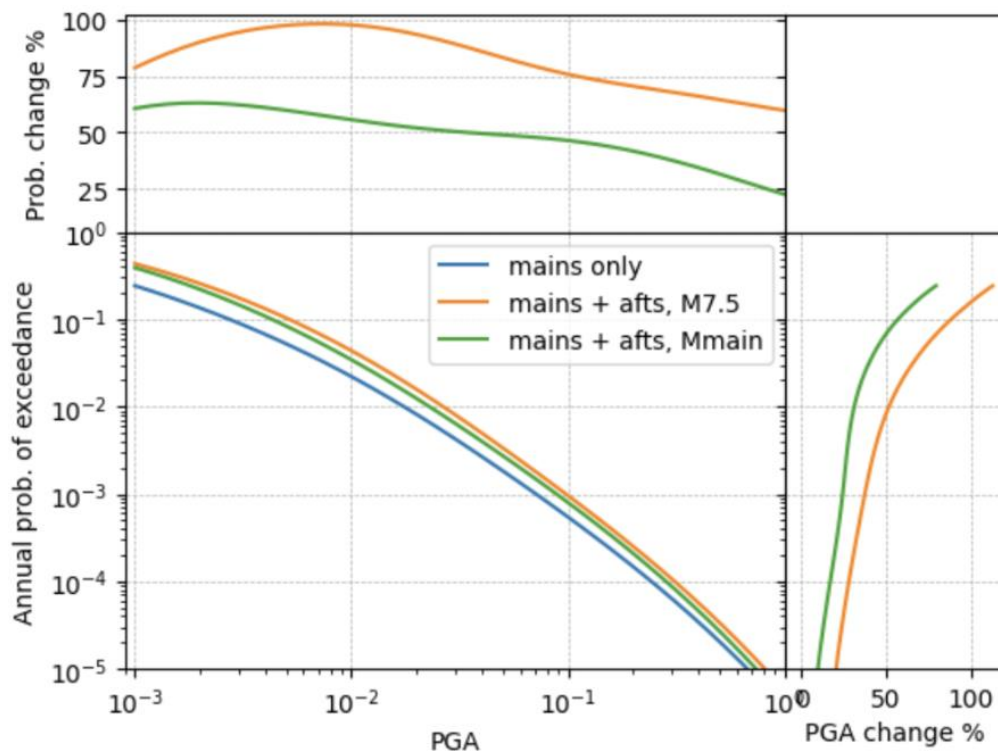


Figure 6 - Hazard curves for the METIS test site, considering three scenarios: The mainshock-only hazard curve is shown in blue. The scenario with the aftershock $M_{\max} = 7.5$ for all sequences is shown in orange. The scenario with the aftershock $M_{\max} = M_{\text{main}}$ is shown in green.

2.5. Checking and Validation of Probabilistic Seismic Hazard Analysis (D4.5)

2.5.1. Research Motivation

PSHA model hazard estimates are a direct input to the probabilistic safety analysis for nuclear facilities. Seismic probabilistic safety analysis is used in the design and optimization of new Nuclear Power Plants (NPPs), as well the continued optimization, monitoring, and maintenance of operational NPPs. Therefore, to provide the 'best-available' information for risk-informed decision making PSHA model testing needs to be an integral part of model development workflow as part of a sequence of iterations toward improving the hazard model.

Both the importance of testing PSHA models and the challenges associated with this testing are well established (Gerstenberger et al., 2020, and references therein). In general, the testing of estimates of recurrence of an earthquake process at a single site is not feasible due to the limited time window of direct and/or indirect ground motion measurements. To overcome the issue of data paucity, it is usually necessary to trade space for time and utilise observed exceedances of ground motion across many sites to provide a dataset large enough to calculate the fit of models to data for return periods of engineering relevance. This space-time trading, referred to as the ergodic assumption, was adopted during WP4.5.

2.5.2. Innovative Aspects of Research Completed

WP4.5 of the METIS project worked to quantitatively compare the results of alternative seismic hazard models for a region, as well as assess whether the PSHA model estimates are consistent with observed ground motions (see Weatherill et al., 2024). To deliver these objectives, PyPSHATest was created in WP4.5, which is an open-source Python toolkit for quantitative

model-to-model and model-to-observation comparison probabilistic seismic hazard results (<https://gitlab.pamretd.fr/openmetis/pypshtest>). The software features various modules for comparisons, both at the level of the components of a seismic hazard model and the outputs. The public availability of this code represents an important step forward in the implementation of PSHA testing as an integral part of the PSHA model development workflow. In addition, the quicktoimplement scripts and run time of PyPSHATest provides PSHA developers with the ability to readily investigate specific assumptions to understand their impact on hazard results.

The first set of PyPSHATest tools were developed to perform model-to-model comparisons, to quantitatively understand the differences in seismic hazard for a site and/or a specific region. Conventionally, PSHA testing has been limited to comparison against a single hazard model or mean seismic hazard map, rather than considering epistemic uncertainty represented by the distribution of hazard curves. Importantly, these PyPSHATest tools provide not only the absolute increase or decrease in means hazard but also differences or inter-quartile range ratios of the total probability distribution. These tools will be valuable during PSHA model development to compare updated versions of a model, when models contain regions that overlap, or when during site specific PSHA modelling, such as for NPPs, multiple models have been developed and an integrator is required to evaluate and assess the models.

The second set of PyPSHATest tools were developed to perform model-to-data comparisons, to quantitatively assess the consistency of PSHA model estimates with direct observations of ground motion, i.e., recorded by instrumentation. One of the most innovative features of the PyPSHATest toolkit, is the 'data imputation by mixed effects regression' that was developed to overcome the issue of ground-motion data incompleteness. Here, existing ground-motion models (GMMs) are used to substitute ground-motion estimates for the missing observed data. Importantly the residual (difference between GMM estimate and observed ground-motions) is decomposed into the between-event residual for earthquakes and the site-to-site residual for stations. This separating of residuals also has the benefit of reducing aleatory variability relative to that of a fully ergodic GMM.

Of particular significance, is that the PyPSHATest model-to-data comparison tools provide the means to investigate the impact of the degree of ergodicity in GMM variability on the known systematic overestimation of hazard, relative to observational ground-motion data. As the ergodic component of variability in the GMMs is removed, PyPSHATest demonstrates that the observed exceedance curves come into closer agreement with the mean and median curves of the hazard models. Therefore, the PyPSHATest tools offer the means to investigate this pattern of model-to-data comparisons in the transition from ergodic to non-ergodic PSHA, which will support the future aim of reconciling observations and estimates of exceedance of ground motions.

2.5.3. Application of Research and Lesson Learned

The PSHA testing approaches innovated in WP4.5 were not applied to a site-specific case study location, due to the necessity of the ergodic compiling of observed exceedances of ground motion at many sites. However, given the necessity to consider earthquakes and their associated ground motions within a large region around a nuclear installation, the testing methods implemented by PyPSHATest can still be informative for a site-specific nuclear installation study. The model-to-model comparison tools were applied to a region along the France-Germany border where three existing PSHA models overlap: Drouet et al. (2020) for metropolitan France, Grünthal et al. (2018) for the 2016 National Seismic Hazard Model for Germany [DE2016], and the ESHM20 (Danciu et al. 2021) for Europe. Figure 7 shows the novel metrics applied in this real-world application, to quantify the model-to-model divergence in distributions of seismogenic sources and resulting exceedance of ground motion.

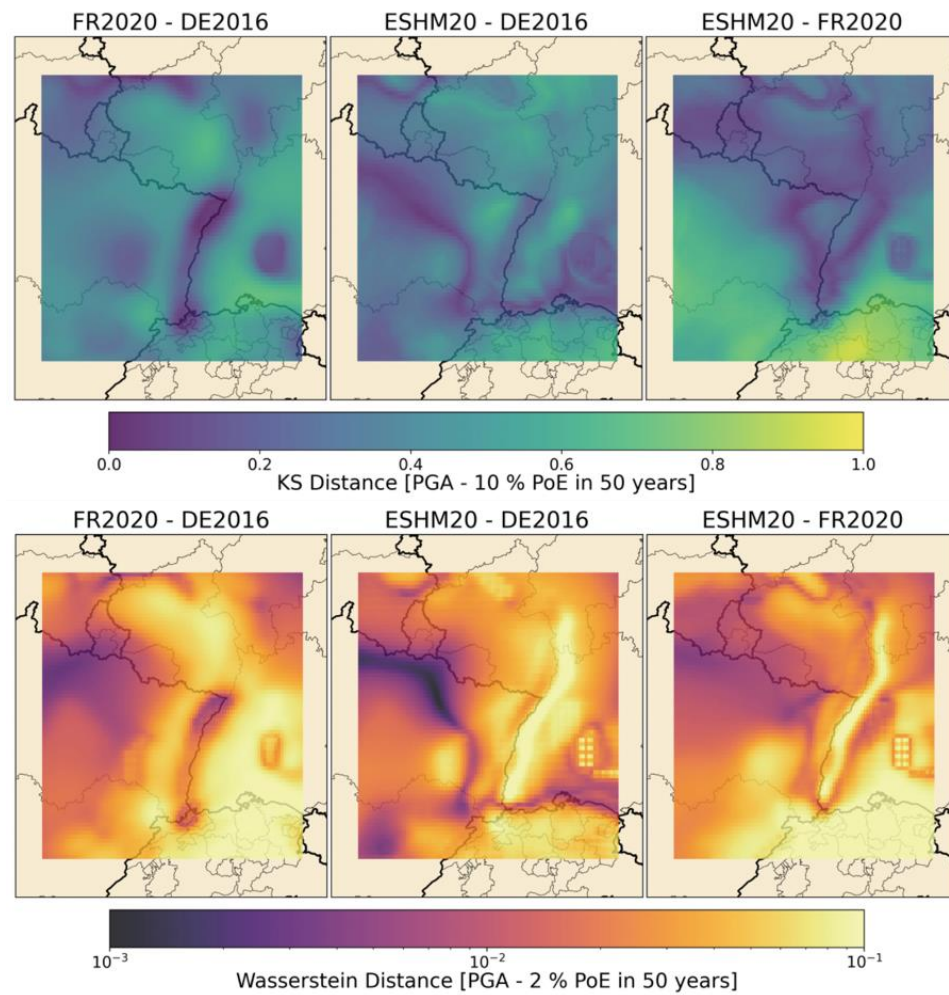


Figure 7 - Comparison of the hazard distribution at the France-Germany border in terms of Kolmogorov-Smirnov distance (top) and Wasserstein Distance (bottom).

The ESHM20 and Drouet et al. 2020 PSHA models were also used in the application of the PyPSHATest model-to-data comparison tools for metropolitan France. While the relatively few earthquakes and recorded ground motions of engineering significance in France, as a results of the low-to-moderate seismicity of the region, may present a challenge for the quantitative comparison of PSHA against observations. However, the use of PyPSHATest demonstrates how the limited data available can still be used for quantitative comparisons against PSHA models.

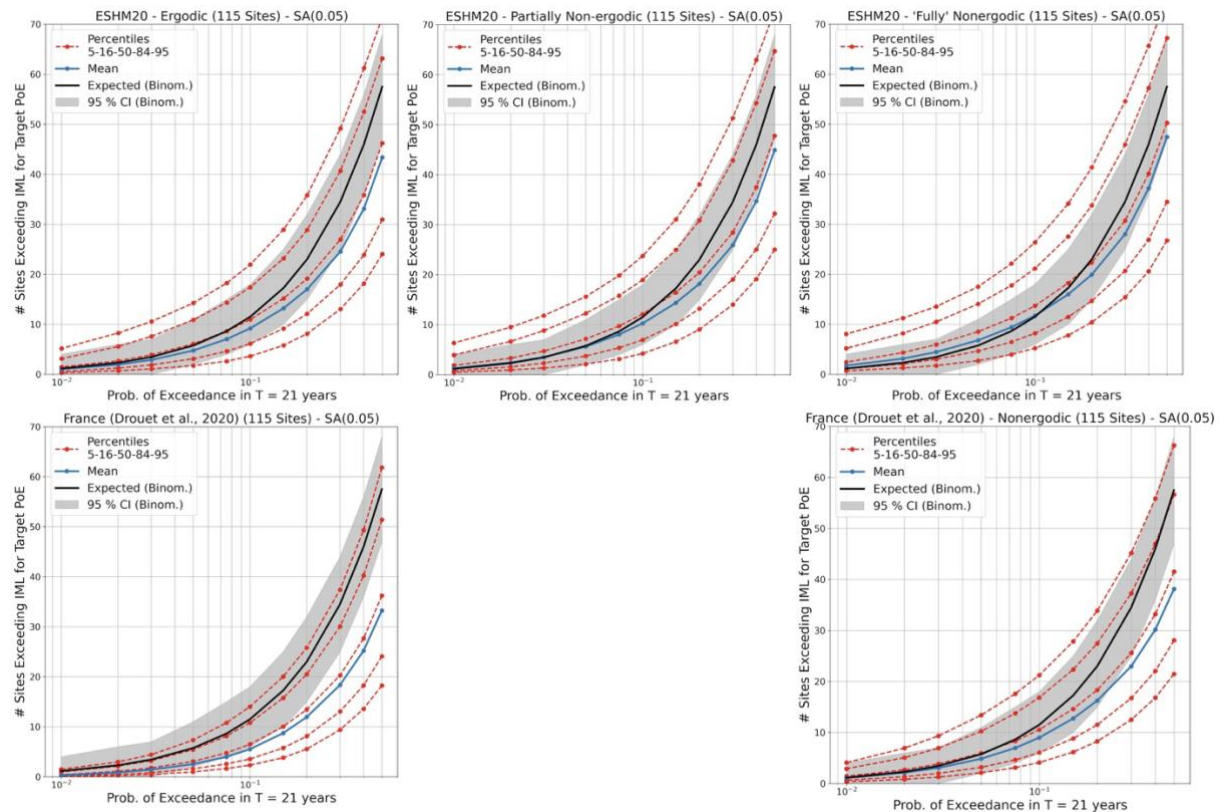


Figure 8 - Comparison of aggregated seismic hazard curves (blue line for the mean hazard and red dashed lines for the quantiles) and the number of stations exceeding their threshold level according to their set probability and the Binomial distribution with expectation (black line) and 5 – 95 % confidence intervals (grey shaded region). Results are shown for SA(0.05) for the PSHA models ESHM20 (top row) and Drouet et al., 2020 (bottom row) using ergodic (left columns), partially non-ergodic (centre column, ESHM20 only) and “fully” non-ergodic variability (right).

3. Conclusions

We summarised the main methodological contributions to seismic hazard modelling proposed within the METIS project, highlighted the most innovative aspects of each of the methodologies proposed with a focus on their application for site-specific studies.

Many of the contributions described open new possibilities for characterising the expected levels of shaking in a more comprehensive way. These include for example the various approaches for physics-based simulation, and the methods for computing vector-valued PSHA.

The newly developed methodology for the propagation of epistemic uncertainty offers opportunities for improving the efficiency of hazard calculation and for incorporating a more articulated set of epistemic uncertainties.

The research completed in Task 4.1 and 4.3 (see Sections 2.1 and 2.6 in this deliverable) introduces new methods for implementing component of the seismic source and ground-motion characterisations and – ultimately – for developing more advanced PSHA input model.

D4.7 PSHA Guidelines



Finally, section 2.5 describes a comprehensive approach for checking PSHA against actual seismicity that can be used while building a hazard model to test the performance of various components and – a posteriori – to prospectively appraise the performance of a hazard model previously released.



4. Bibliography

Ameri G., Shible H. & Baumont D. (2024) Simulation of region-specific ground motions at bedrock by combining spectral decomposition and empirical Green's functions approaches. Accepted for publication on Bulletin of Earthquake Engineering

Bommer, J. J., Coppersmith K., J., Coppersmith R., T., Hanson, K. L., Mangongolo, A., Neveling, J., Rathje, E. M., Rodriguez-Marek, A., Scherbaum, F., Shelembed, R., Stafford, P. J., & Strasser, F. O. (2015). A SSHAC Level 3 Probabilistic Seismic Hazard Analysis for a New-Build Nuclear Site in South Africa. *Earthquake Spectra*, 31(2), 661–698. <https://doi.org/10.1193/060913EQS145M>

Chartier, T. and M. Pagani (2022). Seismic source characterizations methodologies and applications. Deliverable 4.1, METIS project, 30 pages.

Danciu, L., Nandan, S., Reyes, C., Basili, R., Weatherill, G., Beauval, C., Rovida, A., Vilanova, S., Sesetyan, K., Bard, P. Y., Cotton, F., Wiemer, S., & Giardini, D. (2021). The 2020 update of the European Seismic Hazard Models—ESHM20: Model Overview [EFEHR Technical Report 001 v1.0.0]. <https://doi.org/10.12686/a15>

Drouet, S., Ameri, G., Le Dortz, K., Secanell, R., & Senfaute, G. (2020). A probabilistic seismic hazard map for the metropolitan France. *Bulletin of Earthquake Engineering*, 18(5), 1865–1898. <https://doi.org/10.1007/s10518-020-00790-7>

Goulet, C. A., Bozorgnia, Y., Abrahamson, N. A., Al Atik, L. A., Atkinson, G. A., Graves, R., Kuehn, N., & Youngs, R. R. (2019). *NGA-East: A Ground Motion Characterization Model for Central and Eastern North America*. 12th Canadian Conference on Earthquake Engineering.

Grünthal, G., Stromeyer, D., Bosse, C., Cotton, F., & Bindi, D. (2018). The probabilistic seismic hazard assessment of Germany—Version 2016, considering the range of epistemic uncertainties and aleatory variability. *Bulletin of Earthquake Engineering*, 16(10), 4339–4395. <https://doi.org/10.1007/s10518-018-0315-y>

IAEA - International Atomic Energy Agency. (2022). "Seismic Hazards in Site Evaluation for Nuclear Installations". IAEA Safety Standards Series No. SSG-9 (Rev. 1), IAEA, Vienna.

Lavrentiadis, G., Abrahamson, N.A. (2023). A non-ergodic spectral acceleration ground motion model for California developed with random vibration theory. *Bull Earthquake Eng.* 21, 5265–5291. <https://doi.org/10.1007/s10518-023-01689-9>

Lavrentiadis, G., Abrahamson, N.A., Nicolas, K.M. et al. (2023). Overview and introduction to development of non-ergodic earthquake ground-motion models. *Bull Earthquake Eng.* 21, 5121–5150. <https://doi.org/10.1007/s10518-022-01485-x>

NRC - Nuclear Regulations Commission. (1997). NUREG/CR 6372, "Recommendations for Probabilistic Seismic Hazard Analysis: Guidance on Uncertainty and Use of Experts." Washington, DC: U.S. Nuclear Regulatory Commission.

NRC - Nuclear Regulations Commission. (2018). NUREG-2213, "Updated Implementation Guidelines for SSHAC Hazard Studies." Washington, DC: U.S. Nuclear Regulatory Commission.

Pagani, M., T. Chartier, A. Rood (2023). Application to METIS study case (WP4). Deliverable 4.6, METIS project, 36 pages.

Pagani, M., R. Styron, K. Johnson, M. Simionato (2024). New PSHA methodologies: code developments and documentation. Deliverable 4.4, METIS project, 76 pages.

Weatherill, G., F. Cotton, G. Daniel, I. Zentner (2024). Report and code developments for PSHA testing. Deliverable 4.5, METIS project, 90 pages.



Zentner, I., T. Akazawa, L. Alvarez Sanchez, G. Ameri, D. Baumont, F. Cotton, K. Irikura, M. Pilz, H. Razafindrakoto, L. Saint Mard, H. Shible, K. Somei (2023). Physics-based simulation of ground motion tools and database. Deliverable 4.3, METIS project, 109 pages.

5. Datasets and tools

Various dataset produced within the METIS project and cited in this document are available at the METIS community on Zenodo (<https://zenodo.org/communities/openmetis/records?q=&l=list&p=1&s=10&sort=newest>). The OpenQuake Engine can be obtained following the instructions available on its GitHub repository at <https://github.com/gem/oq-engine>.



A1. Conditional Aftershock Probabilistic Analysis for the METIS case study

M. Pagani – GEM Foundation

Aftershocks are generally referred to as smaller earthquakes occurring in proximity of a larger event. Although a univocal definition of aftershocks does not exist, there is clear empirical evidence that the seismicity occurring in the aftermath of an earthquake with magnitude of engineering significance, can generate appreciable levels of shaking that – in some instances – should be considered in the seismic design and risk analysis of infrastructures.

As a matter of fact, current engineering practice does not account for the effects of seismicity triggered just after the mainshock since designing components to withstand the actions generated by the mainshock was considered sufficient to offer an adequate level of protection against the effects of aftershocks.

The METIS project has the goal to improve current practices for the probabilistic risk assessment of nuclear facilities with a specific focus on the seismic component. One of the aims of the project is the incorporation of aftershock impact in the assessment of seismic risk for nuclear plants.

In the initial phases of the projects, extensive discussions were devoted to determining the most appropriate approach to account for the contributions of aftershocks while performing the risk assessment of the various components of a nuclear plant. It has been decided that for nuclear facilities, the impact of aftershocks is relevant within the time indispensable to complete a safe shutdown of the plant in response to the occurrence of the mainshock. On average, the time required to complete this process is in the order of a couple of days.

In the METIS work package 4 (denominated 'Seismic Hazard') the GEM Foundation developed an approach to calibrate the declustering algorithms used to remove from earthquake catalogues the events whose existence is considered conditional on the occurrence of a mainshock event and implemented a methodology through which it is possible to incorporate the contribution of aftershocks in a traditional Probabilistic Seismic Hazard Analysis (PSHA). These two approaches – while certainly useful for a broader set of applications – were not directly able to produce the results necessary to assess the extent to which a plant can be safely brought to a shutdown level.

In this appendix we therefore describe the approach devised to produce the results for assessing the impact of aftershocks on nuclear facilities conditional to the occurrence of a mainshock event, that is the calculation of conditional seismic hazard curves.

A1.1. Methodology

The methodology adopted for computing the conditional aftershock PSHA, uses the results of a disaggregation analysis in terms of magnitude and distance to define the position and geometry of the mainshock. The other two components employed for the construction of the aftershock seismic source characterization are a distribution describing the density of aftershocks against the closest distance to the mainshock rupture (Felzer and Brodsky, 2006) and an aftershock rate derived from a combination of the modified Omori law and the Gutenberg-Richter distribution as proposed by Reasenberg and Jones (1989; see their equation 3).

Using the magnitude of the mainshock and information on the hosting seismic source (e.g. magnitude-scaling relationship, upper and lower seismogenic depths) we create the mainshock rupture.

We consider the number and position of the aftershocks around the mainshock rupture as epistemic uncertainties. Using the mean rate of events in the investigation time (in our case –

as previously described – this corresponds to 2 days) provided by a discretized version of the Reasenber and Jones equation and – assuming a Poisson temporal occurrence model – we generate a few aftershocks for each magnitude bin comprised between the minimum magnitude and the magnitude of the mainshock. In a second step, we distribute these aftershock ruptures around the mainshock one using the spatial density of Felzer and Brodsky. In this analysis, we assume the density of aftershocks as a function of distance is isotropic.

A1.2. OpenQuake (OQ) Engine Input Model

The OQ Engine input model for a conditional aftershock PSHA comprises a Seismic Source Characterization (SSC) and a Ground-Motion Characterization (GMC). The SSC consists of several seismic source models (SSMs) each one comprising the possible set of ruptures representing the aftershock sequence for a given mainshock event. The weight assigned to each SSM corresponds to 1 divided by the total number of simulated patterns of aftershocks.

The GMC corresponds to the one used for the calculation of mainshock PSHA as described in the METIS Deliverable 4.6 “Application to METIS study case”. Future developments could consider adopting ground-motion models calibrated on aftershocks (e.g. Abrahamson et al., 2014).

A1.3. Analysis

We compute the conditional aftershock PSHA for the hypothetical site located in Tuscany used in the METIS study case.

The source zone in the long-term seismic hazard model hosting the site is zone TSZ050. This zone has four nodal plane solutions with the same weight. We choose the solution with a strike at 120 degrees and a dip of 60 degrees but opt to set the dip direction towards east (by rotating the strike 180 degrees).

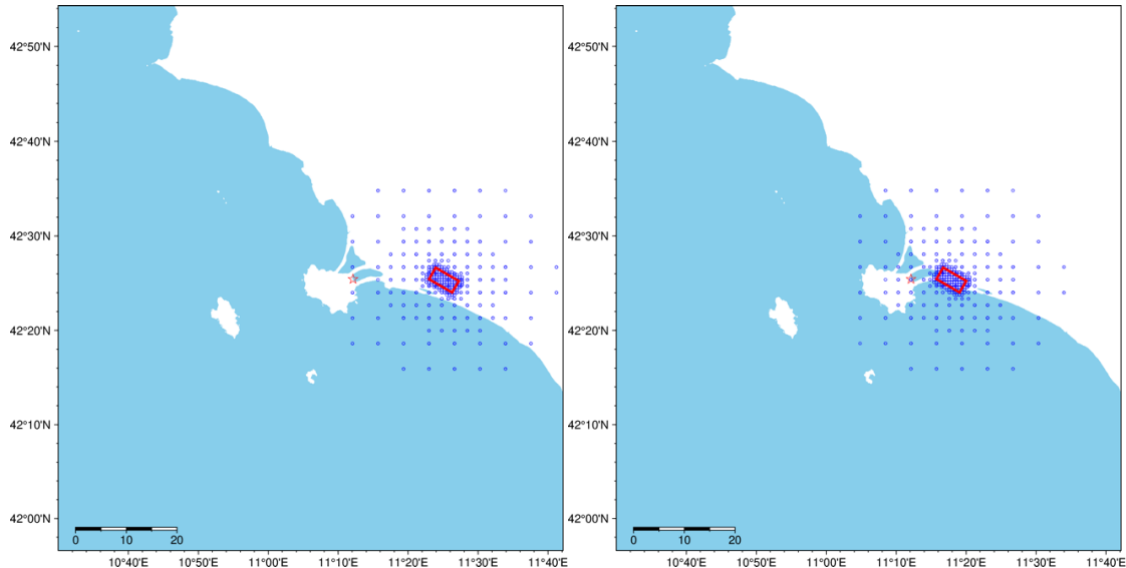


Figure 9 - (left) Mainshock geometry and location for the PGA with return period of 10000 years. (right) Same plot but for the rupture giving the largest contribution to PGA with a return period of 20000 years. The blue dots represent the grid with variable spacing used to distribute the aftershocks around the mainshock rupture.

Then we consider the disaggregation of seismic hazard for PGA with return periods of 10000 and 20000 years. For a return period of 10000 the highest contribution to hazard comes from ruptures located at 15.0 km (closest distance to the rupture) and magnitudes of 5.625. For a return period of 20000 the major contribution comes from magnitudes of 5.625 at 5 km

distance from the site. We choose for these ruptures a depth to the top of rupture of 2 km and a rake of -90 (following the Aki and Richards convention)

Using this information and the parameters assigned to the source TSZ050 we create two rupture geometries representing the mainshock events later used to generate the aftershock sequences. Figure 9 shows the geometry of the rupture representing the mainshock for the PGA with 10000 years return period. The Figure also shows the points of the heterogeneous spacing grid used to create the aftershock ruptures around the mainshock.

Once defined the geometry and position of the mainshock rupture we proceed with the definition of the components required to create the aftershock sequence that is: the total number of aftershocks above the minimum magnitude (4.0 in this case), the magnitude-frequency distribution and the location of the aftershock ruptures with respect to the mainshock one. Figure 9 depicts (in red) the density of aftershocks as a function of the closest distance between the centroid of each aftershock rupture and the surface of the mainshock (see Felzer and Brodsky, 2006; see their Figure 3). The histogram represented with blue dashed lines is the corresponding distribution obtained from the simulated sequences. A good match between the two histograms indicates that the number of samples created provides a good representation of the original distribution.

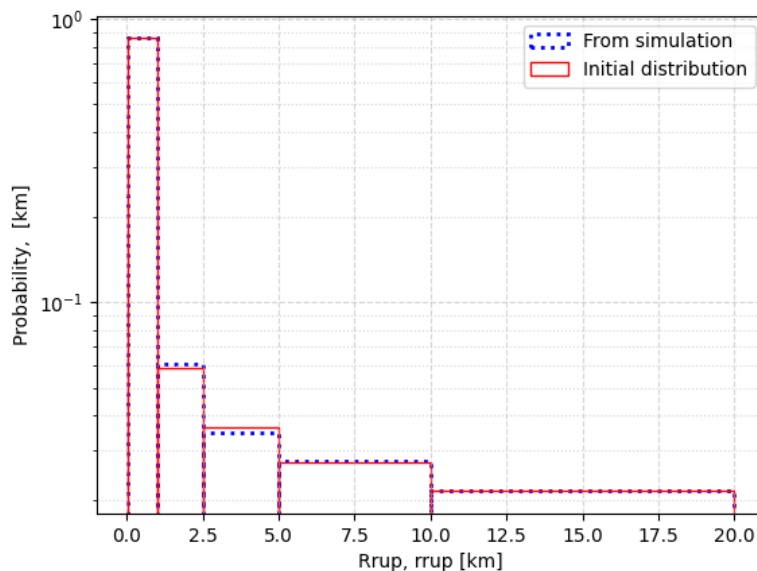


Figure 10 - Density of aftershocks as a function of the closest distance between the centroid of each aftershock rupture and the surface of the mainshock rupture (see Felzer and Brodsky, 2006)

To define the number of aftershocks and their relative magnitudes we use equation 3 of Reasenber and Jones (1998). In accordance with Iervolino et al. (2014), we take the parameters for this equation from Lolli and Gasperini (2003). To create each synthetic aftershock sequence, we sample sequentially these two distributions.

Figure 11 shows two examples of the 175 aftershock sequences simulated for each of the two analyses. The rectangles in black represent the aftershock ruptures while the red box is the mainshock rupture. We store each set of ruptures into one OQ Engine seismic source model. The whole aftershock sequence is described as a non-parametric seismic source where all the ruptures – that is the aftershocks – have a probability of one occurrence in the investigation time of 1.

In addition to the model just described accounting for the epistemic variability in the number and position of ruptures within the aftershock sequence, we also created a mean model that creates ruptures on all the nodes of the grid visible in Figure 9 with rates scaled according to density of aftershocks as represented in Figure 10.

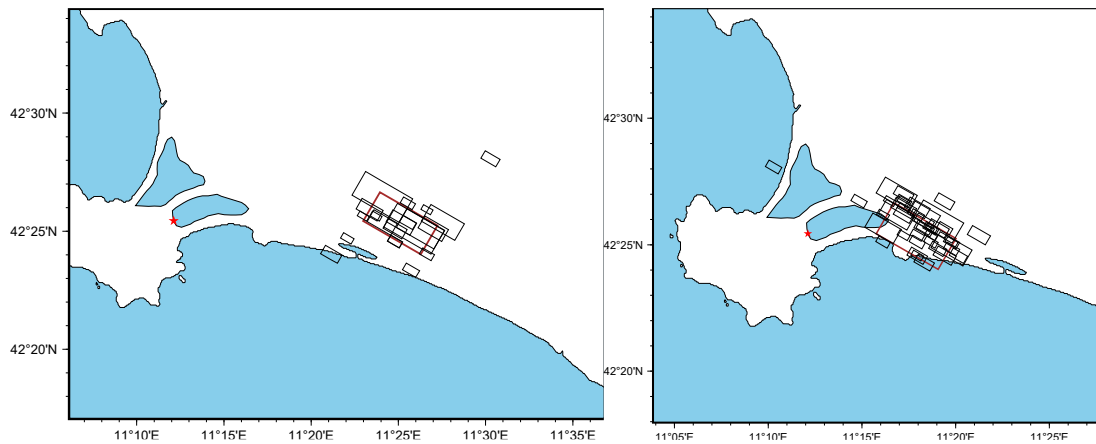


Figure 11 - Aftershock ruptures (in black) and mainshock rupture (red box). The site where we compute the hazard is represented by the red star. (left) Example of simulated aftershock sequence for the rupture giving the largest contribution to PGA with 10000 RP (left) Example of simulated aftershock sequence for the rupture giving the largest contribution to PGA with 20000 RP.

A1.4. Results

Figure 12 shows the 3150 hazard curves admitted by the logic tree devised for the two analyses considered. Not surprisingly, both the plots show an extremely high variability of results (thin green hazard curves). It's also worth to note the large difference in shape between the mean hazard curve and each individual hazard curve; this deviation is well known in the literature (e.g. Abrahamson and Bommer, 2005; see their Figure 1). This difference is even more evident in Figure 13 where the x-axis scales linearly.

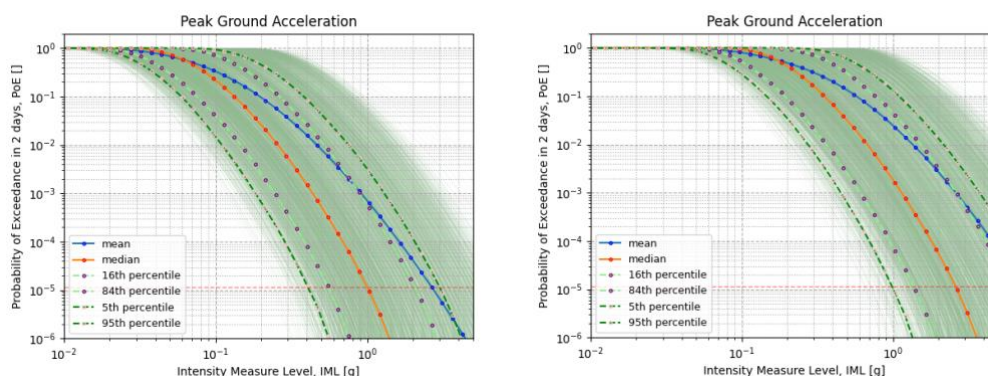


Figure 12 - (left) Seismic hazard curves for the conditional aftershock PSHA analysis computed considering as the mainshock the rupture with the largest contribution to PGA with a return period of 10000 years. (right) Seismic hazard curves for the conditional aftershock PSHA analysis computed considering as the mainshock the rupture with the largest contribution to PGA with a return period of 20000 years.

In Figure 13 we show a comparison between the mean hazard curve obtained by accounting for the epistemic uncertainty in the number and position of ruptures within the aftershock sequence and the mean hazard curve computed using the mean model. In the latter case this variability is considered as being aleatory. The match of the two curves – as expected – is satisfactory.

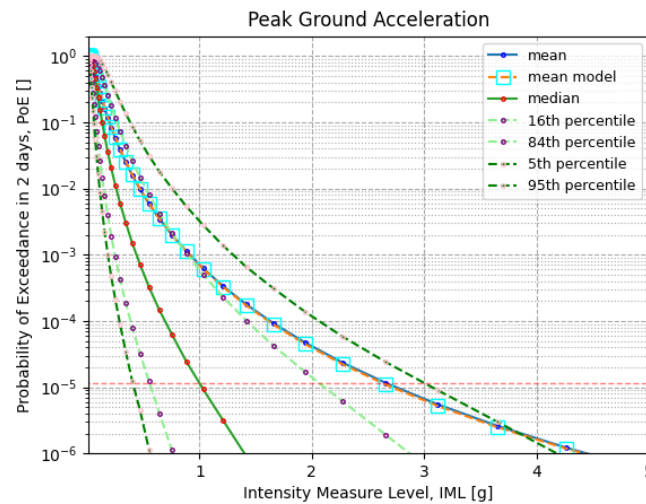


Figure 13 - Comparison between the mean hazard computed with the two conditional aftershock PSHA models for the PGA with a RP of 10000 years. The blue curve represents the mean hazard curve computed considering the number and position of ruptures as epistemic uncertainties. The squares in cyan represent the mean hazard curve computed considering the mean model, where these two components of uncertainty are assumed to be aleatory.

Using the mean model, we also compute the conditional spectra for the investigated site. Figure 14 shows an example of conditional spectrum computed using the mean model generated with the rupture giving the largest contribution to the mainshock hazard for PGA with a return period of 1e4 years. The conditioning period used is PGA.

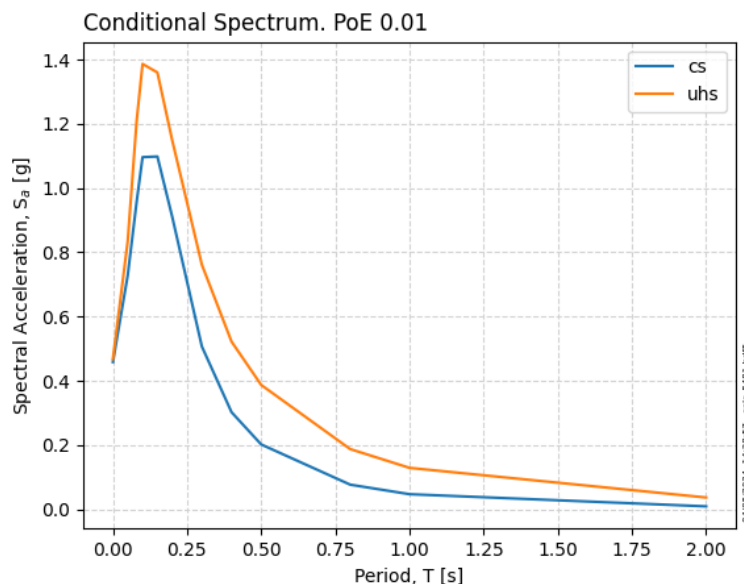


Figure 14 - Conditional spectrum with a 1% probability of being exceeded in the 30 hours used as the investigation time. The model used to compute this is the mean model of aftershocks generated by the rupture with the largest contribution to the mainshock hazard for PGA with a return period of 1e4 years. The conditioning period is PGA.



A1.5. Conclusions

We described the implementation of a methodology for the calculation of hazard due to aftershocks conditional to the occurrence of a mainshock with predefined geometry and magnitude. This information is extracted from the results of the hazard disaggregation analysis for the mainshock hazard.

The approach proposed can either create a mean hazard model based on the assumption that number of aftershocks and their position is an aleatory variability or a model where this uncertainty is treated as epistemic. The latter approach has the power to demonstrate the large variability of hazard results due to the lack of knowledge of how many aftershocks will be generated and their position. The mean hazard curves computed with the two approaches show an almost perfect agreement and can be also considered a way to cross check the two implementations.

In addition to traditional results of a probabilistic analysis of seismic hazard (e.g., hazard curves), using the mean model it is possible with the OQ Engine to compute conditional spectra and therefore obtain a suite of results fully consistent with the one computed with the mainshock hazard.

The methodology proposed is simple and has the advantage of considering the finiteness of the mainshock rupture in defining the spatial distribution of aftershocks. It could be improved in many ways. For example, by using alternative models for the generation of the aftershock sequence (e.g., ETAS-like) or by performing a more appropriate characterisation of the ground motion modelling component.

A1.6. References

- Abrahamson, N. A., & Bommer, J. J. (2005). Probability and Uncertainty in Seismic Hazard Analysis. *Earthquake Spectra*, 21(2), 603–607. <https://doi.org/10.1193/1.1899158>
- Abrahamson, N. A., Silva, W. J., & Kamai, R. (2014). Summary of the ASK14 Ground Motion Relation for Active Crustal Regions. *Earthquake Spectra*, 30(3), 1025–1055. <https://doi.org/10.1193/070913eqs198m>
- Felzer, K. R., & Brodsky, E. E. (2006). Decay of aftershock density with distance indicates triggering by dynamic stress. *Nature*, 441(7094), 735–738. <https://doi.org/10.1038/nature04799>
- Iervolino, I., Giorgio, M., & Polidoro, B. (2014). Sequence-Based Probabilistic Seismic Hazard Analysis. *Bulletin of the Seismological Society of America*, 104(2), 1006–1012. <https://doi.org/10.1785/0120130207>
- Lolli, B., & Gasperini, P. (2003). Aftershocks hazard in Italy Part I: Estimation of time-magnitude distribution model parameters and computation of probabilities of occurrence. *Journal of Seismology*, 7(2), 235–257. <https://doi.org/10.1023/A:1023588007122>
- Reasenber, P. A., & Jones, L. M. (1989). Earthquake Hazard After a Mainshock in California. *Science*, 243(4895), 1173–1176. <https://doi.org/10.1126/science.243.4895.1173>



A2. Application of new approach for epistemic uncertainty propagation to the METIS case study

One of the outcomes of the METIS work package dedicated to seismic hazard was a new methodology for the propagation of epistemic uncertainties (see Pagani et al., 2023). In Appendix we present the results computed for the METIS case study computed using this new method for the propagation of epistemic uncertainty.

Figure 15 shows a comparison between the hazard curves computed using directly the OpenQuake Engine and the ones obtained using this new approach for the propagation of epistemic uncertainty. The plot a) shows the comparison between the mean hazard curve computed with the OQ Engine and from the set of histograms representing the distribution of the probability of exceedance using all the sources included in the hazard model. Plot b) shows the same comparison but only considering the results obtained using the zone encompassing the site, that is TSZ050. This is the zone that controls almost entirely the hazard at the site.

Overall, the performance of the methodology proposed and its implementation appears successful although further improvements and tests will be added to check a possible error leakage for very low values of shaking (not of engineering relevance).

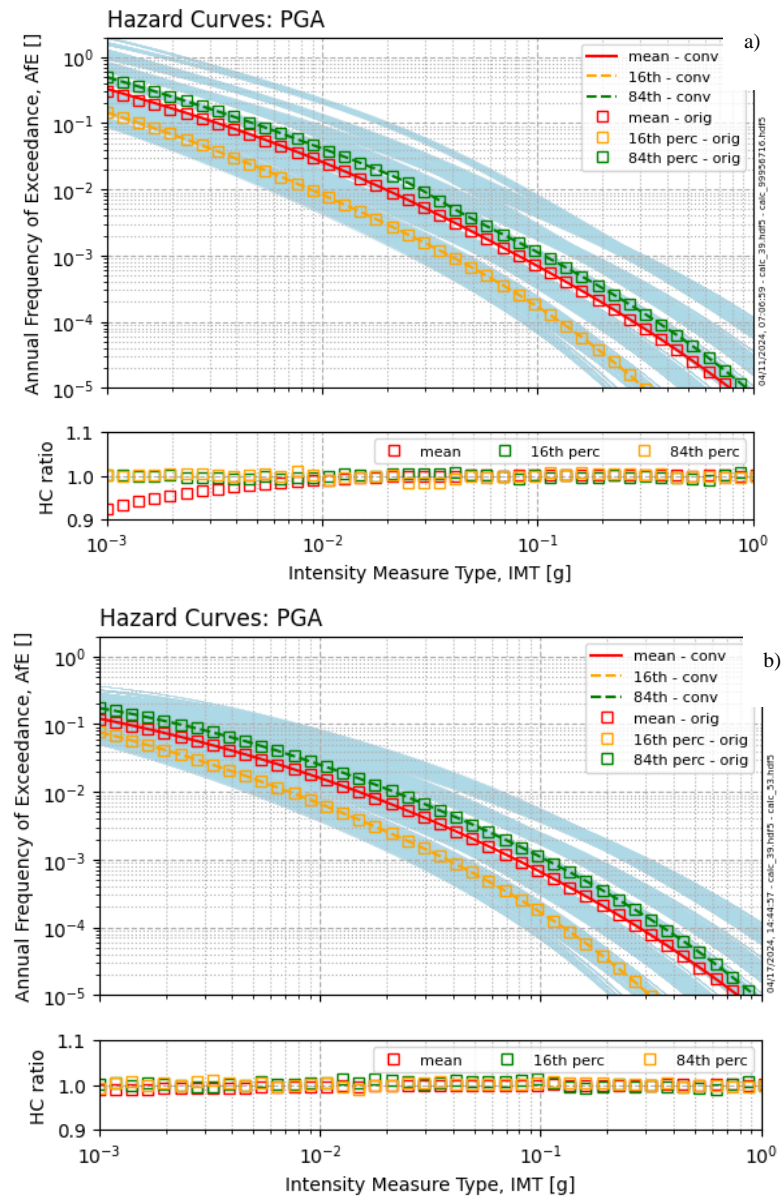


Figure 15 - Comparison between the mean, 16th and 84th percentile hazard curves for PGA representing the annual frequency of exceedance at the METIS test site as obtained from the OpenQuake Engine with the traditional calculation approach and the with the new approach proposed for the propagation of epistemic uncertainty. In both plots the lower panel shows the comparison between the ratio of the original result over the corresponding one computed using the new approach proposed. [a] Comparison computed considering all the sources [b] Comparison computed considering only the area source encompassing the site TSZ050.